

Design of High Efficiency Circular Horn Feeds for Multibeam Reflector Applications

Kwok Kee Chan and Sudhakar K. Rao

Abstract—Design aspects of high efficiency profiled circular horns with thin walls as feeds for multibeam reflector antennas for satellite applications are presented in this paper. The modal content at the circular aperture of the horn necessary to closely approximate a unipolarized uniform distribution is first established. Slope discontinuities along the length of the horn are then used to generate the necessary aperture modes with the appropriate amplitudes and phases. The performance of the horn is calculated using the mode matching technique. Significant improvement in the horn aperture efficiency and reduction in the cross-polar level over a straight conical horn can be achieved over a single band or two bands that are widely separated in frequency. This conclusion is supported by the good agreement between predictions and measurements of a high efficiency dual-band horn.

Index Terms—Horn antennas, mode matching methods, multibeam antennas, reflector antenna feeds, satellite antennas.

I. INTRODUCTION

For satellite communications, there is a need to provide multibeam coverage at both uplink and downlink frequency bands. The antenna of choice is a reflector (either parabolic or shaped surface) fed by multiple horns, with each horn forming a single beam. In contrast to reflector antennas with a single feed, the aperture size of these horns is restricted and is determined by the adjacent beam spacing, number of reflectors, and the reflector geometry [1]. The efficiency of the horn plays a major role in the performance of multiple beam antennas (MBA). Higher efficiency of the horn results in improved edge-of-coverage and improved copolar isolation among beams that re-use the same frequency. Conventional solutions proposed in the literature [6], [7] employ either corrugated hard-horn geometry or use of dielectric materials and are not suitable for multibeam space applications due to thicker walls that increase mass and lower the antenna efficiency or due to electro-static discharge (ESD) associated with use of dielectrics in space. The design approach presented in this paper is different from the traditional methods of improving the aperture efficiency of the reflector antenna through the use of thin metallic wall construction of the multimode horn feed. Ludwig [2] synthesizes the modes in the single circular horn feed to give an approximately uniform illumination of the reflector in order to get maximum peak gain from the secondary beam. Here, we are interested in improving the edge-of-coverage or beam cross-over gain and are not overly concerned with the peak gain, as well as reducing the sidelobes. Typically in a multibeam reflector design, where the horn size is determined by the beam spacing, the only way to improve the performance of the MBA system is to increase the horn efficiency. Increased efficiency of these horns produces narrower primary patterns that result in reduced spill-over, and increased illumination taper on the reflector. This results in increased edge-of-coverage gain and lower sidelobe levels for the secondary patterns. It was shown earlier [1], [3], [4] that the edge-of-coverage gain improvements of the order of 1 dB to 2 dB could be achieved for the secondary beams by increasing the horn

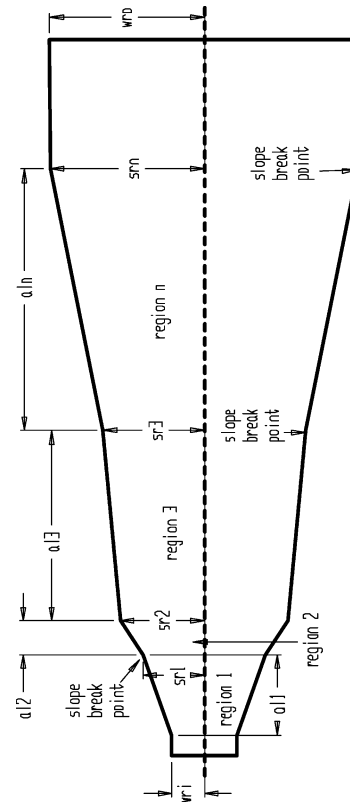


Fig. 1. Multimode profiled horn.

efficiency. Further, the co-polar sidelobes are lowered, thus increasing the inter-beam isolation. The efficiency of these horns can be improved by introducing the appropriate kind and level of higher order modes at the horn aperture by means of circularly symmetric discontinuities along the horn. These discontinuities take the form of slope changes so that a smooth profiled horn results as shown in Fig. 1. The success of this approach has been verified by the close agreement between predictions and measurements of a high efficiency dual-band horn. From our numerical experiments, it is found that for a given aperture size, slope discontinuity gives higher aperture efficiency over a broader band than for step discontinuity used in [5].

The steps necessary for the successful design of a multimode circular horn are as follows.

- a) Determine the ideal modal content at the horn aperture, given the desired distribution;
- b) Synthesize a profiled horn to give the desired radiation characteristics, such as bandwidth, aperture efficiency, return loss, and peak cross-polar levels, by means of optimization of horn physical parameters. Performance prediction is carried out using the mode matching technique.

These steps are discussed below.

II. DETERMINATION OF APERTURE MODAL CONTENT

The horn aperture electric field distribution $f(r, \phi)$ may be written as a summation of the orthonormalized transverse waveguide propagating mode vectors e_i as $f(r, \phi) = \sum A_i \bar{e}_i$. The coefficients A_i of the circular waveguide modes are given by

$$A_i \propto \int_0^{2\pi} \int_0^b f(r, \phi) \hat{x} \cdot \bar{e}_i r dr d\phi \quad (1)$$

Manuscript received February 11, 2007; revised August 1, 2007.
 K. K. Chan is with Chan Technologies Incorporated, Brampton, ON L6Y 5H1, Canada, (e-mail: kwok-kee.chan@rogers.com).
 S. K. Rao is with Lockheed Martin Commercial Space Systems, Newtown, PA 18940 USA.
 Color versions of one or more of the figures in this paper are available online at <http://ieeexplore.ieee.org>.
 Digital Object Identifier 10.1109/TAP.2007.913172

TABLE I
CIRCULAR WAVEGUIDE TE_{1n} AND TM_{1n} MODES

Mode	χ , root	Guide diameter (λ)
TE_{11}	1.841183	0.5861
TM_{11}	3.831706	1.2197
TE_{12}	5.331443	1.6971
TM_{12}	7.015587	2.2331
TE_{13}	8.536316	2.7172
TM_{13}	10.17346	3.2383
TE_{14}	11.70601	3.7261
TM_{14}	13.32369	4.2411
TE_{15}	14.86359	4.7312
TM_{15}	16.47062	5.2428
TE_{16}	18.01553	5.7345

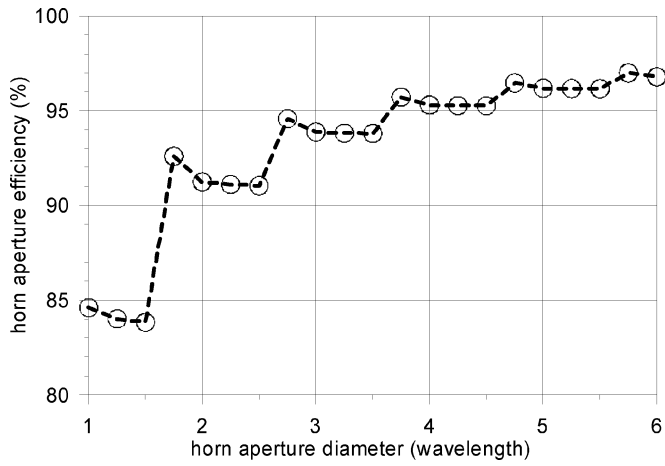


Fig. 2. Maximum achievable aperture efficiency of circular horn with multiple TE_{1n} modes approximating uniform aperture distribution.

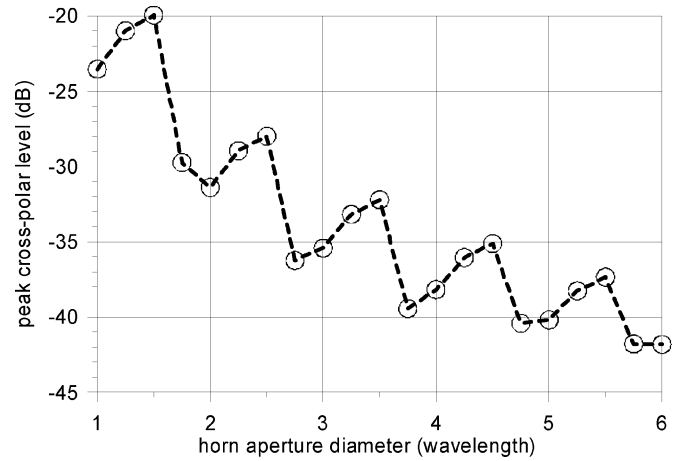


Fig. 3. Peak cross-polar level of maximum aperture efficiency circular horn.

where $i = (m, n)$ is the mode index, and (r, ϕ) are the cylindrical coordinates. The aperture distribution is assumed to be perfectly polarized in the \hat{x} -direction. The integration is taken over the horn aperture with radius b . The type of distribution of interest to us here is uniform i.e., $f(r, \phi) = 1$ for maximum efficiency.

It is assumed that the horn is fed by a single-moded guide with the TE_{11} mode. All the discontinuities are circularly symmetric. Consequently only the TE_{1n} and TM_{1n} modes can be excited. A list of these modes, together with the roots of their characteristic equations and the horn diameters where they are above cutoff, are given in Table I. The x -components of these modes are given as follows:

TE_{1n} modes

$$e_{ix}^h = \sqrt{\frac{2}{\pi}} \sqrt{Z_i^h} \frac{\chi_i^h}{\left[(\chi_i^h)^2 - 1 \right]^{1/2} b J_1(\chi_i^h)} \times \left\{ \frac{J_1\left(\frac{\chi_i^h r}{b}\right)}{\frac{\chi_i^h r}{b}} \cos^2 \phi + J_1'\left(\frac{\chi_i^h r}{b}\right) \sin^2 \phi \right\} \quad (2)$$

TM_{1n} modes

$$e_{ix}^e = \sqrt{\frac{2}{\pi}} \sqrt{Z_i^e} \frac{1}{b J_0(\chi_i^e)} \left\{ \frac{J_1\left(\frac{\chi_i^e r}{b}\right)}{\frac{\chi_i^e r}{b}} \sin^2 \phi + J_1'\left(\frac{\chi_i^e r}{b}\right) \cos^2 \phi \right\}. \quad (3)$$

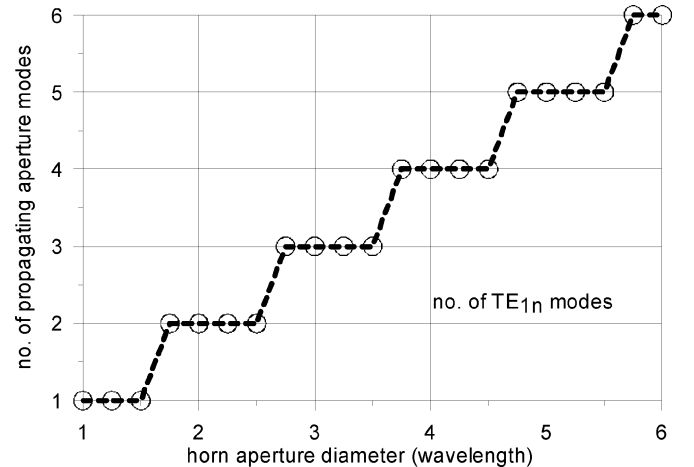


Fig. 4. Number of propagating TE modes at the aperture of maximum efficiency circular horn.

Here, b is the guide radius, χ/b is the mode cutoff wavenumber, Z_i is the mode impedance, $J_n(x)$ is the Bessel function of the first kind of order n and argument x , and the prime associated with the Bessel function denotes the first derivative with respect to the argument. The maximum horn aperture efficiency and minimum cross-polar level that can be achieved by a circular aperture with no phase error and the

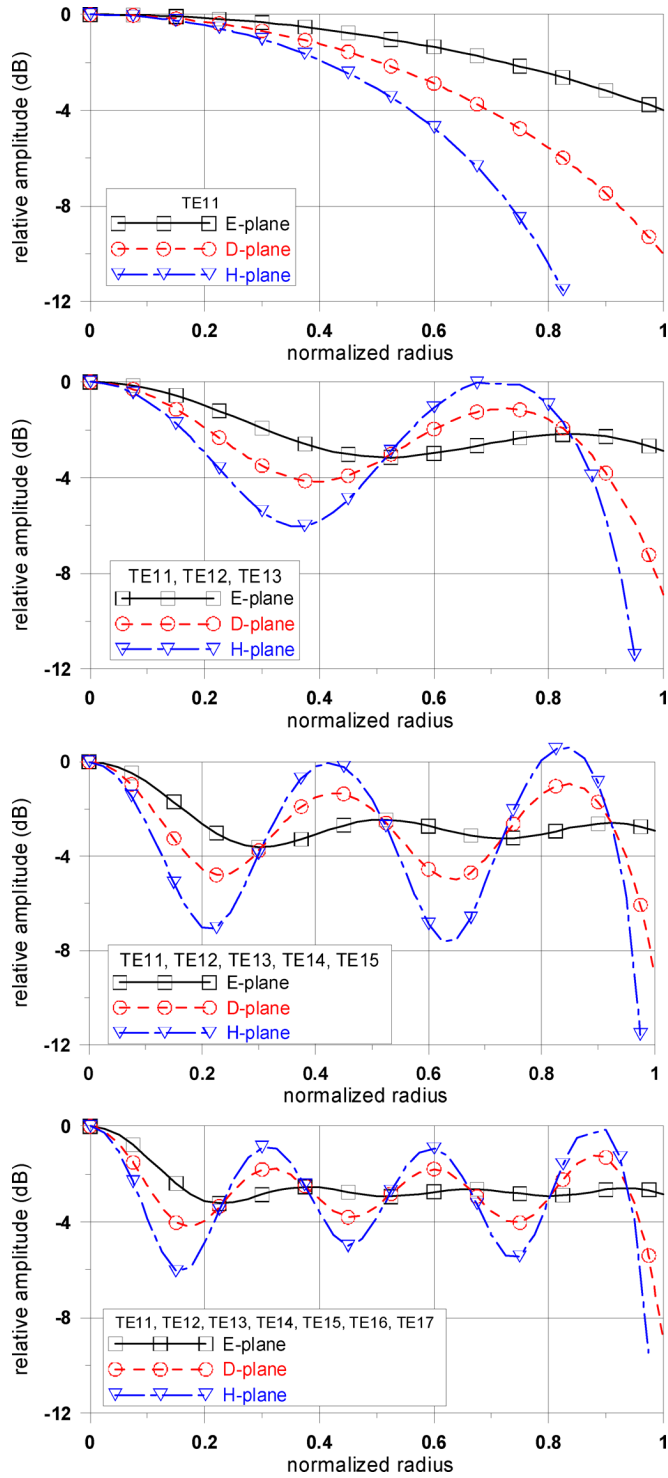


Fig. 5. Aperture distributions of a horn with 1, 3, 5, and 7 TE modes.

corresponding modal content should first be established. Aperture efficiency is defined here as the ratio of the peak copolar directivity and the maximum directivity from the same aperture with uniform amplitude and phase distributions. The directivity patterns of the horn aperture were computed from the aperture modal content using Kirchoff's vector diffraction integral [8]. The theoretically maximum aperture efficiency and peak cross-polar level, together with the number of propagating modes with non-zero excitations are plotted in Figs. 2–4, respectively as a function of aperture diameter in wavelength. It should

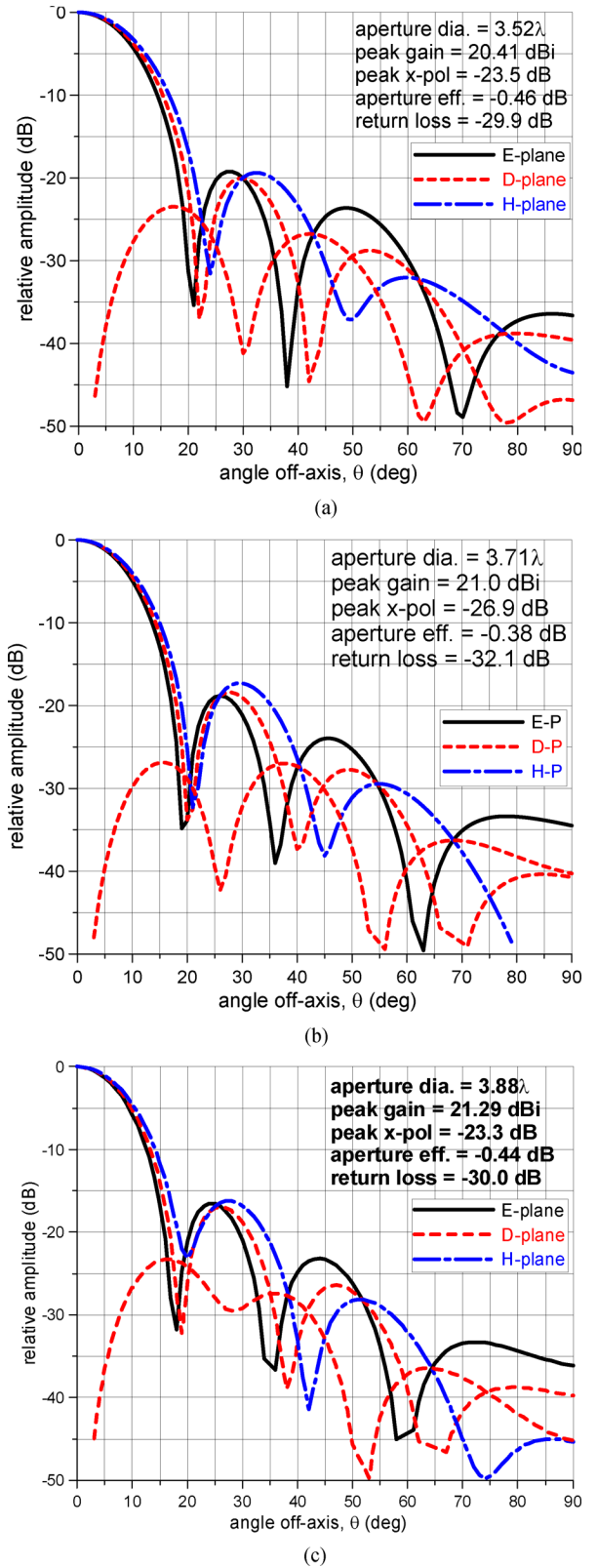


Fig. 6. Radiation pattern cuts of a single band high efficiency horn at (a) 18.3 GHz, (b) 19.3 GHz, (c) 20.2 GHz.

be noted that in Fig. 4, the number of propagating modes to approximate a uniform distribution is shown. For the unpolarized uniform distribution, only the TE_{1n} modes are needed. This is in contrast to that of a feed horn designed to produce a high efficiency reflector antenna where both TE_{1n} and TM_{1n} modes are required in the horn [2].

TABLE II
MODAL CONTENT OF SINGLE BAND HIGH EFFICIENCY CIRCULAR HORN WITH 3.71λ APERTURE DIAMETER

Mode	Ideal Modal Content		Actual Modal Content	
	Amp (V)	Phase (deg)	Amp (V)	Phase (deg)
TE ₁₁	1.0	0.0	1.0	0.0
TM ₁₁	0.0	0.0	0.0205	+25.5
TE ₁₂	0.3112	0.0	0.2813	-11.4
TM ₁₂	0.0	0.0	0.0376	-132.5
TE ₁₃	0.2202	0.0	0.0557	+36.3
TM ₁₃	0.0	0.0	0.0238	+25.2

However, if a tapered distribution is specified for the horn aperture, both TE_{1n} and TM_{1n} modes are needed. The staircase nature of these plots is caused by the presence of an increasing number of higher order modes, as these modes can only propagate at certain aperture diameters as given in Table I. Thus for a given aperture size, there is a maximum aperture efficiency that can be achieved due to the available number of propagating TE_{1n} modes. This can be seen in Fig. 5 where the E-, D-, and H-plane cuts ($\phi = 0, 45, \text{ and } 90 \text{ deg.}$, respectively) of the horn aperture distribution are plotted for different number of TE modes. It can be seen that an increasing number of TE modes leads to a more uniform distribution with reduced ripple level. One can also achieve good cross-polar performance together with high aperture efficiency. The peak cross-polar level can be further reduced by sacrificing a bit of aperture efficiency by introducing an amplitude taper. For the results shown in these plots, only TE_{1n} modes are present in the proper proportions. No TM_{1n} modes exist at the aperture. The achievability of such a condition in practice is investigated next.

III. SYNTHESIS OF PROFILED CIRCULAR HORNS

The method chosen here to excite the higher order modes employs slope discontinuity. This approach is found to have broader bandwidth performance than utilizing step discontinuity. Slope discontinuity is better at minimizing the level of the unwanted TM modes. The structure of a profiled horn with multiple discontinuities is shown in Fig. 1. The horn profile is linear in between the discontinuities. It is not possible to generate the TE modes without exciting the TM modes with a circular discontinuity. In practice, one can aim to control the excitation of one or two higher order TE modes and minimize the excitation of the TM modes. Since only one or two higher order TE modes need to be generated and controlled in either one or two frequency bands, using 3 or 4 slope discontinuities should suffice. The discontinuity count excludes the one at the interface with the single moded input guide.

The design process involves (see Fig. 1) specifying the approximate axial locations (al) of the slope break points and the radii (sr) of the horn cross-sections at these break points. These breakpoints are set by the number of higher order modes with significant power. The specified horn profile is then segmented into a series of stepped circular waveguide sections with varying radii. Size of the waveguide step is typically less than 0.02λ . The horn performance is characterized by finding the generalized scattering matrices (GSM) of all the stepped waveguide junctions and then combining them together with those of the intervening waveguide sections to yield the overall scattering parameters. With the modal content at the aperture known, the radiation patterns can be readily calculated. If the input return loss, peak cross-polar level and the efficiency of the horn are worse than the desired values at the

specified frequencies ($i = 1, nfrq$), then they are used to form the objective function F which is given as

$$F = \sum_{i=1}^{nfrq} \{ wt_r(\rho_i - \rho_{di})^2 + wt_x(xp_i - xp_{di})^2 + wt_a(\eta_i - \eta_{di})^2 \} \quad (4)$$

here, ρ , xp , and η represent the return loss, peak cross-polar level in the diagonal plane, and aperture efficiency, respectively. All these parameters are expressed in dB and the subscript d indicates the desired value. The corresponding weights of the error functions are wt_r , wt_x , and wt_a . It should be noted that the weightings are set so that the error components are more or less of the same magnitude. An optimization routine minimizes the above objective function by searching for the optimum radii and locations of the slope breakpoints. This search is carried out within the limits of the optimization variables that are set by the user.

IV. RESULTS

Simulations were carried out to determine how close one could achieve the theoretical aperture efficiency limits shown in Fig. 2 by using a 3.71λ diameter horn at 19.30 GHz. This horn has a 10.4% frequency bandwidth. The ideal and actual aperture modal contents achieved are tabulated in Table II. Gain pattern cuts are plotted in Fig. 6 at the band edge and center frequencies. The theoretical maximum efficiency is 94%. The best achievable efficiency is 91.6% at band center, which is close to the theoretical limit, and 90% and 90.4% at the lower and upper band edge respectively. Such good efficiency is achieved by having close to the required level of TE₁₂ mode and keeping the levels of the TM modes low.

Next to be investigated is a dual band horn, with the low band centered at 19.3 GHz and the high band centered at 29.2 GHz. The horn has four slope discontinuities, an aperture diameter of 5.766 cm and an axial length of 17.78 cm. For the optimization of this horn, the values of wt_r , wt_x , and wt_a used are 1, 1, and 200, respectively. The desired values for ρ_{di} , xp_{di} and η_{di} in (4) are -25 , -24 and -0.7 dB. The horn is divided into 228 waveguide sections. The ideal and realized aperture modal contents are shown in Table III. The resulting amplitude and phase distributions are plotted in Figs. 7 and 8 at 19.3 GHz and 29.2 GHz. The aperture distribution is more or less in phase at the low band and has small phase errors at the high band. It is difficult to get close to the required levels of higher order TE_{1n} modes in the two widely separated bands. However, we are able to maintain a low level of TM modes. Consequently the aperture efficiency is not as high as

TABLE III
APERTURE MODAL CONTENT OF DUAL BAND HIGH EFFICIENCY CIRCULAR HORN

Mode	Low band aperture content				High band aperture content			
	Ideal		Actual		Ideal		Actual	
	Amp (V)	Phase (°)	Amp (V)	Phase (°)	Amp (V)	Phase (°)	Amp (V)	Phase (°)
TE ₁₁	1.0	0.0	1.0	0.0	1.0	0.0	1.0	0.0
TM ₁₁	0.0	0	0.0743	35.7	0.0	0	0.1567	45.1
TE ₁₂	0.3112	0	0.0308	47.3	0.3016	0	0.2088	-44.0
TM ₁₂	0.0	0	0.0298	12.7	0	0	0.0691	38.6
TE ₁₃	0.2202	0	0.0202	-57.5	0.1946	0	0.0205	-106.7
TM ₁₃	0.0	0	0.0262	82.7	0.0	0	0.0220	95.2
TE ₁₄	Cutoff	-			0.1532	0	0.0063	-48.0
TM ₁₄	Cutoff	-			0.0	0	0.0197	58.6
TE ₁₅	Cutoff	-			0.1428	0	0.0014	-119.2
TM ₁₅	Cutoff	-			0.0	0	0.0031	127.8

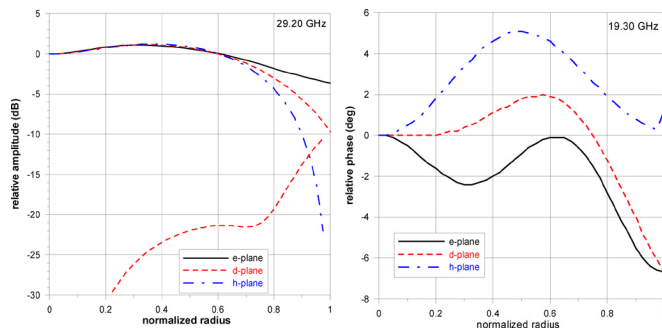


Fig. 7. Amplitude and phase distributions across the aperture of the dual-band horn at 19.3 GHz.

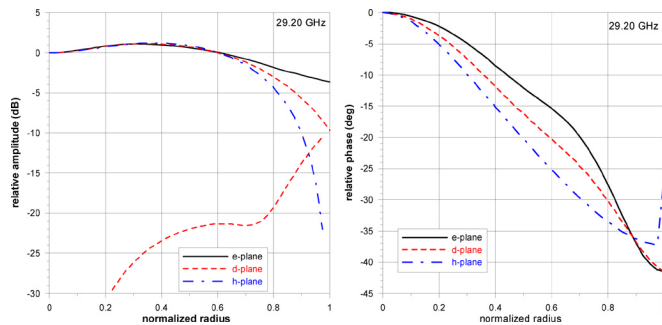


Fig. 8. Amplitude and phase distributions across the aperture of the dual-band horn at 29.2 GHz.



Fig. 9. Breadboard model of the dual-band horn.

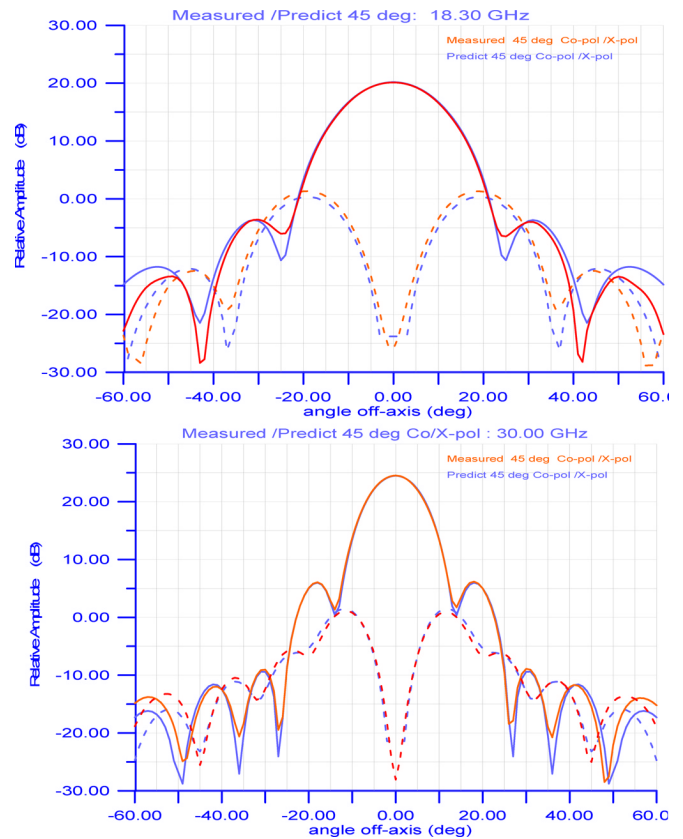


Fig. 10. Comparison between computed and measured gain patterns of the dual-band horn.

that of the single band horn but we are able to get a remarkable efficiency in the mid-eighties in both bands. Fig. 9 shows the breadboard horn that covers both the *K* and *Ka* bands. The wall thickness of the horn at the aperture region is 0.5 mm. The measured versus computed radiation patterns of the horn are shown in Fig. 10. There is an excellent correlation between the two. A comparison of the predicted and measured performances is shown in Table IV. A minimum efficiency value of 84% to 85% is achieved across the *K/Ka* band frequencies. Measured return loss is better than 25 dB and compares well with the predictions as seen in Fig. 11. Peak cross-polar levels are between -20

TABLE IV
COMPARISON OF PREDICTED AND MEASURED PERFORMANCES OF DUAL-BAND HORN.

Frequency (GHz)	Directivity (dBi)/ Efficiency		Peak Cross-Pol (dB)	
	Predict	Measured	Predict	Measured
18.30	20.08 (83.4%)	20.10 (83.8%)	19.8	18.8
19.30	20.60 (84.5%)	20.60 (84.5%)	20.5	20.5
20.20	21.05 (85.6%)	21.1 (86.6%)	20.6	20.7
28.30	23.89 (83.9%)	23.9 (84.0%)	24.1	23.1
29.20	24.23 (85.2%)	24.2 (84.6%)	26.0	24.2
30.00	24.46 (85.1%)	24.5 (85.9%)	23.0	24.4

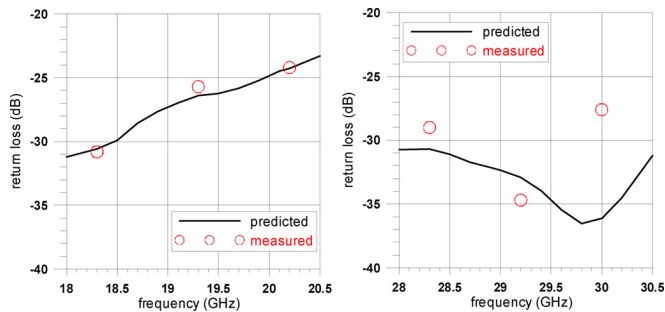


Fig. 11. Computed and measured return loss of the dual-band horn.

to -26 dB relative to copolar peak and they agree well with computations. These primary cross-polar levels translate to better than 23 dB cross-polar isolation for the secondary beams with an offset reflector. These levels easily meet the inter-beam cross-polar isolation requirement of 18.8 dB (axial ratio of 2 dB) for the multiple beam satellite antennas. We have also developed a feed network that supports two orthogonal polarizations at both K -band and Ka -band, while achieving better than 60 dB isolation between the bands, and better than 24 dB return loss with the high efficiency horn attached. For comparison, a same size conventional conical horn has an aperture efficiency of 76% and a peak cross-polar level of -17.5 dB. Also same size Potter and corrugated horns would have 70% and 52% aperture efficiency values respectively. A significant increase in aperture efficiency has thus been achieved. By employing the high efficiency horn as the feed, it was shown in [3], [4] that the multibeam antenna RF performance in terms of gain and copolar isolation can be significantly increased resulting in doubling the satellite capacity when compared to conventional feed horns. The K/Ka dual-band high efficiency horn is typically fed with a compact feed assembly that fits behind the real-estate dictated by the horn aperture. Such a feed assembly consists of a symmetrical OMT junction, band reject filters, polarizers, matching network, and transitions and has been already developed by Lockheed Martin.

V. CONCLUSION

This paper presents the design of a high-efficiency circular horn with plain wall construction that is highly desirable for multiple beam reflector antennas for use in satellite communications. Design results agree well with the measurements for a dual-band high efficiency horn that operates at the K and Ka -band frequencies.

REFERENCES

- [1] S. Rao and M. Q. Tang, "Stepped-reflector antenna for dual-band multiple beam satellite communications payloads," *IEEE Trans. Antennas Propag.*, vol. 54, no. 3, pp. 801–811, Mar. 2006.
- [2] A. C. Ludwig, "Radiation pattern synthesis for circular aperture horn antennas," *IEEE Trans. Antennas Propag.*, vol. 14, pp. 434–440, Jul. 1966.
- [3] S. Rao, K. K. Chan, and M. Tang, "Dual-band multiple beam antenna system for satellite communications," presented at the IEEE Antennas Propagation Int. Symp., Washington, DC, Jul. 3–5, 2005, Session 84.
- [4] S. Rao, M. Tang, and Lockheed Martin, "Multiple-Beam Antenna System Using High-Efficiency Horns," U.S. patent Application 11/029390, Oct. 29, 2004.
- [5] A. K. Bhattacharyya and G. Goyette, "A novel horn radiator with high aperture efficiency and low cross-polarization and applications in arrays and multibeam reflector antennas," *IEEE Trans. Antennas Propag.*, vol. 52, no. 11, pp. 2850–2859, Nov. 2004.
- [6] P. S. Kildal and E. Lier, "Hard horns improve cluster feeds of satellite antennas," *Electron. Lett.*, no. 24, pp. 491–492, 1988.
- [7] S. Skobelev and P. S. Kildal, "Modal solutions in dual-depth longitudinally corrugated waveguides for design of dual-band 20/30 GHz hard horns," in *Proc. IEEE Antennas Propagation Int. Symp.*, Jul. 2006, pp. 1211–1214.
- [8] S. Silver, "Microwave antenna theory and design," *MIT Rad. Lab. Ser.*, vol. 12, pp. 336–338, 1949.